Heliyon 10 (2024) e24379

Contents lists available at ScienceDirect

Heliyon

journal homepage: www.cell.com/heliyon

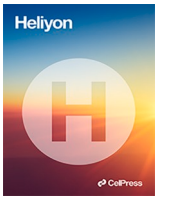

Research article

Comparison of MUSE-DWI and conventional DWI in the application of invasive breast cancer and malignancy grade prediction: A comparative study

Weicheng Wang [a], Bowen Dou [a], Qi Wang [b], Haogang Li [b], Changshuai Li [b], Wenjing Zhao [b], Longjiang Fang [b], Dmytro Pylypenko [c], Yujing Chu [b,*]

[a] Weifang Medical University, Weifang, 261053, China
[b] Department of Radiology, Weifang People's Hospital, Weifang, Shandong, 261041, China
[c] Magnetic Resonance Research, GE Healthcare, Beijing, China

ARTICLE INFO

Keywords:
Invasive breast cancer
MUSE-DWI
Diffusion-weighted imaging
Image quality
Diagnostic efficacy

ABSTRACT

Objective: To compare MUSE-DWI with conventional DWI in assessing lesions of invasive breast cancer and evaluating the ADC values for preoperative histological grading.
Methods: A retrospective analysis was conducted on 63 lesions confirmed as invasive breast cancer by surgical or biopsy pathology. Preoperatively, all patients underwent MUSE-DWI, conventional DWI, and dynamic contrast-enhanced (DCE) scans. Two radiologists with over 5 years of experience (intermediate and senior levels, respectively) subjectively evaluated the images for clarity, image artifacts, and distortion. Objective evaluation included signal-to-noise ratio (SNR) of lesions and fibrous tissue, as well as the ADC values of both imaging techniques. Due to the limited number of cases classified as grade I and the insignificant difference in disease-specific survival and recurrence scores between grades I and II tumors, grades I and II were grouped as low-grade, while grade III was classified as high-grade. Receiver operating characteristic (ROC) curves were used to evaluate the efficacy of ADC values in preoperatively predicting the grading of invasive breast cancer.
Results: The SNR and subjective quality scores of MUSE-DWI images were significantly higher than those of conventional DWI ($p < 0.05$). For the same case, the ADC values of MUSE-DWI were lower than those of conventional DWI. The AUC values for predicting the grading of invasive breast cancer were 0.849 for MUSE-DWI and 0.801 for conventional DWI.
Conclusion: Compared to conventional DWI, MUSE-DWI significantly reduces artifacts and distortions, greatly improving image quality. Moreover, MUSE-DWI demonstrates higher diagnostic efficacy for preoperative histological grading of invasive breast cancer.

1. Introduction

Breast cancer is the leading cause of fatal cancer in women, accounting for 30 % of all newly diagnosed cancers and 15 % of deaths in women, and clinical treatment and prognosis vary widely among different breast cancer patients [1]. Breast cancer is a highly heterogeneous tumor, and its histopathological grading is considered an independent prognostic factor in imaging [2]. Histological

* Corresponding author. 151 Guangwen Street, Kuiwen District, Weifang City, China.
E-mail address: chuyujing2023@126.com (Y. Chu).

https://doi.org/10.1016/j.heliyon.2024.e24379
Received 9 August 2023; Received in revised form 20 December 2023; Accepted 8 January 2024
Available online 18 January 2024

grading has been demonstrated as a biological surrogate model for cancer in various malignancies [3,4]. The Nottingham histological grading system is currently the internationally recognized system for grading breast cancer. This system comprehensively evaluates the proportion of infiltrating ductal carcinoma, cellular pleomorphism, and mitotic count to determine an objective histological grade [5]. Moreover, the Nottingham grading system is closely associated with early recurrence and shorter survival rates, independent of tumor size, hormone receptor status, or lymph node metastasis [3,6]. Consequently, the latest 8th edition of the American Joint Committee on Cancer (AJCC) breast cancer staging system has incorporated Nottingham grading as an important component of tumor staging [7]. Therefore, histopathological grading of invasive breast cancer is crucial.

Currently, obtaining histopathological grading for invasive breast cancer mainly relies on invasive procedures such as surgical excision or biopsy [5]. However, these invasive procedures have limitations in terms of patient discomfort, safety concerns, and accessibility to certain patient populations. Magnetic resonance imaging (MRI) possesses high soft tissue resolution and is useful for distinguishing between benign and malignant breast lesions [8]. Various MRI techniques, including quantitative MRI with relaxation properties, Chemical Exchange Saturation Transfer (CEST) MRI, and Dynamic Contrast-Enhanced (DCE) imaging, have been proposed for the detection of breast cancer. Meng T. et al. explored the diagnostic efficiency of quantitative mapping in patients with breast cancer. They discovered that quantitative T1 and T2 values obtained through SyMRI could effectively differentiate between benign and malignant breast lesions, with the T1 relaxation time exhibiting the highest diagnostic efficiency [9]. Moreover, combining both values enhanced diagnostic proficiency. Additionally, Schmitt et al. performed breast examinations on female patients with invasive ductal carcinoma using a 3.0T MRI scanner [10]. They observed that the regions with high signal intensity in CEST imaging correlated well with the tumor areas depicted by DCE-MRI. While these studies yielded encouraging results, they primarily focused on distinguishing between benign and malignant breast lesions or tumor imaging correlation. Limited work was performed in malignancy grade prediction.

Diffusion-weighted imaging (DWI) is a promising non-contrast MRI technique for breast cancer detection [11,12]. By calculating

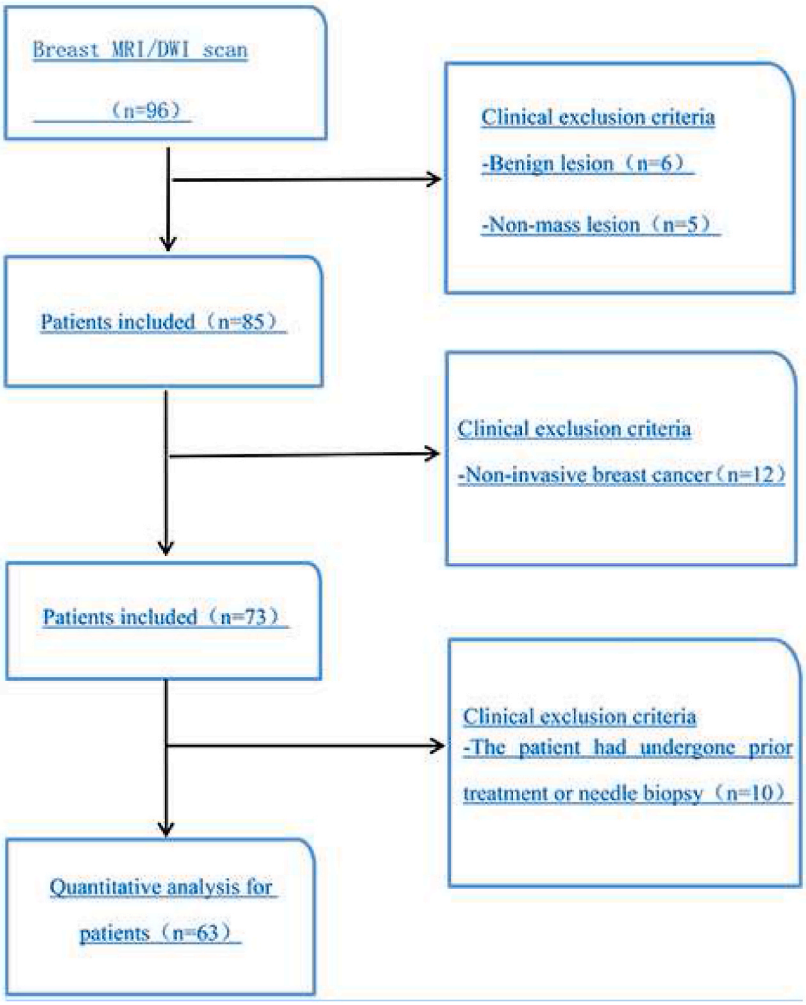

Fig. 1. Patient selection workflow.

the ADC values, it is possible to quantitatively determine the nature of the lesions [13]. However, DWI images obtained using single-shot echo-planar imaging (SS-EPI) are limited by artifacts, resulting in relatively low spatial resolution that averages the lesions with surrounding normal breast tissue, leading to image blurring [14]. Traditional DWI techniques only involve morphological analysis of lesions, and different pathologies may exhibit similar imaging appearances due to artifacts and distortions, affecting radiologists' observation and analysis of lesion morphology.

Multiple sensitivity encoding DWI (MUSE-DWI) is a multi-channel segmented echo-planar imaging technique that extends the existing sensitivity encoding by utilizing interleaved trajectory k-space to achieve higher signal-to-noise ratio (SNR) and improved spatial resolution without the need for navigational pulses [15]. MUSE-DWI has been applied in various areas such as breast, abdomen, hippocampal sclerosis, endometrial cancer, and prostate cancer [15–18]. Based on these applications, researchers have found that MUSE-DWI offers higher SNR, image clarity, lower deformation, and image artifacts compared to traditional DWI techniques, leading to better visualization of lesion morphology. Isaac et al. investigated the utility of diffusion-weighted imaging with multiplex sensitivity coding in the identification of breast lesions and found that it exhibited a degree of diagnostic efficacy [15]. However, the small sample size limited the exploration of the full potential of MUSE-DWI. Given these promising results, it warrants further investigation to determine whether a more robust performance in the diagnostic efficacy of MUSE-DWI can be achieved for histological grading of invasive breast cancer.

Therefore, our research aims to observe the value of comparing MUSE-DWI and SS-EPI-DWI in the visualization of invasive breast cancer and compare their effectiveness in predicting the malignancy grade. This will provide a basis for the enhancement of predictive diagnostic efficacy for invasive breast cancer by combining multiple techniques or multimodal MRI with MUSE-DWI."

2. Materials and methods

2.1. General information

The institutional review board approved our retrospective study and waived the need for written informed consent. We conducted this study in compliance with the Health Insurance Portability and Accountability Act. A retrospective collection was performed on 63 female patients diagnosed with invasive breast cancer confirmed by invasive biopsy or surgical pathology at Weifang People's Hospital between November 2022 and April 2023. The patients' ages ranged from 26 to 73 years, with an average age of (51.56 ± 10.54) years. The inclusion and exclusion criteria are shown in Fig. 1. Our study aimed to focus on mass-invasive breast cancer; therefore, individuals with benign lesions or non-mass breast cancer were not included in the dataset. Additionally, patients should not have undergone treatment or biopsy before the MRI, as this may lead to the lesion not accurately reflecting the actual situation, resulting in distorted ADC measurements.

2.2. Instruments and methods

All MRI experiments were performed on a 3.0T MRI scanner (SIGNA™ Architect, software version DV29.0, GE), with a dedicated 8-channel phased-array coil for breast imaging. Patients were positioned prone, with both breasts naturally hanging inside the coil and both arms raised and placed on the sides of the head. Feet first positioning was used, and the reconstruction of images for b = 0s/mm2 and b = 1000s/mm2 was automatically completed. MUSE-DWI: TE78.2 ms, matrix256 × 256 , FOV 36mm × 40.3 mm, slice thickness 5 mm, scanning time 209s, excitation frequency 2, number of slices 28,bValues 0,1000 s/mm^2. SS-EPI-DWI: TE 79.1 ms, matrix 256 × 256, FOV 36mm × 40.3 mm, slice thickness 5 mm, scanning time 148s, excitation frequency 1, number of slices 28, b Values 0,1000 s/mm^2. The specific scanning parameters are shown in Table 1.

2.3. Image analysis

Two physicians with 5–10 years of experience, respectively, in breast MR diagnosis jointly analyzed the images and performed subjective evaluations. When two physicians had a disagreement, a consensus was reached through discussion. Employing a 4-point scale, the two physicians independently assessed the image clarity, distortion, and artifacts across all DWI sequences, while remaining

Table 1
Scanning parameters of MUSE-DWI and conventional DWI.

Parameter	MUSE-DWI	SS-EPI-DWI
Repetition time (ms)	6796	9436
Echo time TE (ms)	78.2	79.1
matrix	256 × 256	256 × 256
FOV (mm)	36 × 40.3	36 × 40.3
Slice thickness (mm)	5	5
Scanning time (s)	209s	148s
Slice spacing (mm)	1	1
b Value (s/mm^2)	0 , 1000	0,1000
Excitation frequency	2	1
Number of slices	28	28

blind to each other's evaluations. The rating scale for image clarity was as follows: 4 points for clear lesion visualization with sharp and clear depiction of the surrounding glands, 3 points for clear lesion visualization with slightly lower contrast with the surrounding glands, 2 points for acceptable visualization of the lesion and surrounding glandular tissue with poor contrast, and 1 point for acceptable visualization of the lesion with blurry surrounding glandular tissue. The rating scale for artifacts was as follows: 4 points for no artifacts, 3 points for minimal artifacts, 2 points for moderate artifacts, and 1 point for significant artifacts. Image deformation was assessed by measuring the transverse and anteroposterior diameters of the lesions in the two DWI sequences compared to the DCE images. The absolute difference in diameters was calculated, and scores were assigned as follows: $\leq$2 mm for no visible deformation (score 4), >2 mm and $\leq$4 mm for mild deformation (score 3), >4 mm and $\leq$6 mm for moderate deformation (score 2), and >6 mm for severe deformation (score 1). If the absolute differences in the anteroposterior and transverse diameters fell into different score categories, the lower score was used for analysis.

SNR measurement: Regions of interest (ROIs) were identified within the images containing the tissues or structures of interest. The average signal intensity of the ROI was measured. In the same image, ROIs containing only background noise, such as the external body region or signal-free area, were identified. The standard deviation of the signal intensity within the background ROI was measured. The SNR was calculated using the formula SNR = average signal intensity/standard deviation of noise. Given the potential impact of parallel acquisition techniques on the measurement of background noise levels, we opted to use locally measured noise within the ROI to estimate the background noise [19]. This approach aims to provide a more accurate representation of the noise characteristics specific to the region of interest, thus enhancing the reliability of our SNR calculations.

Apparent diffusion coefficient (ADC) measurement: MUSE-DWI and SS-EPI-DWI images were imported into the GE AW4.7 workstation, and ADC maps were automatically generated using the vendor provded READY View software. When multiple lesions were present, we selected the largest one, particularly in cases with multiple centers. Using DCE images as a reference, 3D Slicer (https://www.slicer.org, version 5.4.0) was employed to outline the ROI of the lesions, and then Seeit （ www.medaifan.net, version 0.80) software was used to extract the histogram of the ROI region, which is illustrated in Fig. 2A–C. Park et al. [20] proposed that the 50th percentile ADC value was the most promising indicator for distinguishing between ductal carcinoma in situ and invasive ductal cancer, with sensitivity and specificity values of 82.9 % and 75.7 %. Therefore, we roughly took the value of the 50th percentile as the ADC value of the lesion.

2.4. Histological grading

Pathological results were obtained through surgical resection or biopsy within one week after breast MR examination. The Nottingham combined histologic grade (NCHG) was used to histologically grade the invasive breast cancer [5]. Due to the low number of grade I cases and the lack of significant differences in disease-specific survival and recurrence scores between grade I and grade II tumors, grade I and grade II were classified as the low-grade group, while grade III was classified as the high-grade group [21].

2.5. Statistical analysis

Statistical analysis was performed using SPSS version 26.0 software. Normally distributed continuous data were expressed as "x $\pm$ s," and non-normally distributed data were expressed as interquartile range. Paired t-tests were used for parametric tests, and Wilcoxon signed-rank tests were used for non-parametric tests. The intraclass correlation coefficient between the two radiologists was evaluated according to the following interpretation: a value of 0.75–1.00 was considered excellent agreement, 0.60–0.74 was considered good agreement, 0.40–0.59 was considered fair agreement, and less than 0.40 was considered poor agreement [22]. Receiver Operating Characteristic (ROC) curves were used to evaluate the diagnostic performance of ADC values derived from MUSE-DWI and conventional DWI in stratifying the level of invasive breast cancer. The area under the curve (AUC) was calculated. A p-value of less than 0.05 was considered statistically significant.

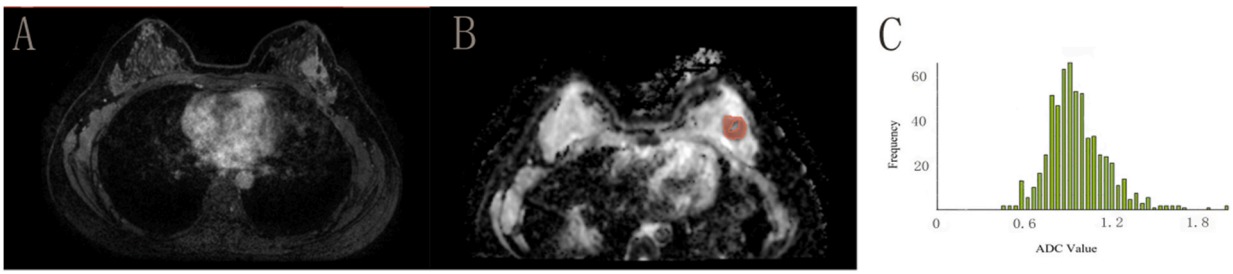

Fig. 2. A 39-year-old patient with grade NOS II invasive breast cancer. On axial postcontrast T1-weighted image, a mild enhanced Breast cancer is located in the left breast (A). Regions of interest (ROIs) were manually drawn encompassing all lesion voxels across multiple slices on apparent diffusion coefficient (ADC) map (B). Note that the necrotic area within the tumor with the lack of enhancement on postcontrast T1-weighted image (A) and high signal intensity on apparent diffusion coefficient (ADC) map (B) is not included in the ROI. (C)An ADC histogram of the entire mass. The ADC values in units of 10^{-6} mm^2/s are as follows: 5th percentile, 0.71; 10th percentile, 0.80; 50th percentile,0.98; 90th percentile, 1.21; 95th percentile, 1.39.

3. Results

3.1. Qualitative results

The interobserver agreement between the two experienced radiologists was robust, with ICC values indicating strong agreement for MUSE clarity (ICC = 0.857), SS-EPI-DWI clarity (ICC = 0.81), MUSE artifacts (ICC = 0.856), SS-EPI-DWI artifacts (ICC = 0.852), MUSE distortion (ICC = 0.709), and SS-EPI-DWI distortion (ICC = 0.883).These results are summarized in Table 2. Regarding image clarity, both radiologists gave higher ratings to MUSE-DWI compared to SS-EPI-DWI ($z = -3.216$, $p < 0.01$; $z = -4.310$, $p < 0.01$). Conversely, MUSE-DWI received lower scores for image artifacts ($z = -4.709$, $p < 0.01$; $z = -3.243$, $p < 0.01$) and distortion ($z = -4.973$, $p < 0.01$; $z = -3.978$, $p < 0.01$) compared to SS-EPI-DWI. These results are summarized in Table 3 and illustrated in Fig. 3A–C,Fig. 4A–C.

3.2. Quantitative results

In terms of SNR, the lesions in the MUSE-DWI group exhibited an SNR of 585.1 ± 224.9, whereas the SS-EPI-DWI group had an SNR of 405.0 ± 168.1. This difference was statistically significant ($p < 0.05$) and is documented in Table 4.

Among the 63 cases of invasive breast cancer, 2 were classified as histological grade I, 33 as grade II, and 28 as grade III. All the lesions demonstrated solid-enhancement morphology. Notably, the ADC values derived from MUSE-DWI (0.82 ± 0.13) were significantly lower than those from SS-EPI-DWI (0.89 ± 0.15) ($p < 0.05$), as presented in Table 5.

3.3. Diagnostic efficacy

Additionally, the ROC curve analysis revealed that the AUC values for predicting the grade grouping of invasive breast cancer were 0.849 for MUSE-DWI ADC values and 0.801 for SS-EPI-DWI ADC values, indicating a statistically significant difference ($p < 0.05$). This data is further detailed in Table 6 and visually represented in Fig. 5.

4. Discussion

In this study, we thoroughly investigated the efficacy of MUSE-DWI in visualizing invasive breast cancer as well as predicting malignancy grade and contrasted it with the conventional SS-EPI-DWI. Our findings affirm that MUSE-DWI delivers superior image clarity and detail, further evidenced by a higher SNR. These insights align with previous studies by Gabrielle [15] and Dimiel [23], endorsing the potential of MUSE-DWI as a pioneering diagnostic tool. Dimiel's study demonstrates that MUSE DWI of breast tumors is feasible and can be easily implemented with a routine breast MRI protocol. Gabrielle thinks the image quality of MUSE-DWI was superior to that of ss-EPI-DWI and geometric distortion and blurring were significantly reduced, although there was an increase in acquisition time. Leveraging MUSE-DWI in multimodal MRI or with other techniques could significantly enhance diagnostic precision, heralding an evolution in invasive breast cancer management.

The results demonstrate that MUSE-DWI images have higher resolution, less distortion, and fewer artifacts. Both qualitative and quantitative results from this study revealed that the performance of MUSE-DWI in terms of image deformation was superior to that of SS-EPI-DWI, and the difference was statistically significant. Upon analyzing the reason behind this, it can be inferred that SS-EPI's slow filling of K-space along the phase coding direction results in widespread geometric distortion. MUSE-DWI employs segmented EPI technology to expedite K-space filling, thereby enhancing image quality [24]. Simultaneously, MUSE-DWI exhibited greater similarity to enhanced T1WI in the depiction and morphological description of lesions.

In comparison to SS-EPI-DWI, MUSE-DWI incorporates sensitivity encoding parallel imaging and optimizes matrix inversion conditions, resulting in a higher SNR and enhanced spatial resolution, as evidenced by previous studies [25,26]. These observations were also reflected in this study. The SNR measured by MUSE-DWI was higher than that measured by SS-EPI-DWI, and the difference was statistically significant. It can be concluded that MUSE-DWI possesses a higher spatial resolution and can significantly improve image quality.

The ADC values obtained from the MUSE-DWI group were lower than those from the SS-EPI-DWI group, and this difference was statistically significant. This can be attributed to the relatively blurry image quality of SS-EPI-DWI, which affects the accurate measurement of ADC values. In essence, the lower resolution of the images leads to an averaging effect within the ROI, blending with adjacent normal fibroglandular tissue, which results in higher measured ADC values. Compared to single-shot DWI, the use of MUSE-DWI enables a clearer and higher-quality visualization of lesions, allowing for a more precise estimation of the histological grade of invasive breast cancer. Additionally, as an important index for evaluating tumor malignancy and grading, ADC values play a significant

Table 2
Consistency of subjective evaluation of MUSE-DWI and SS-EPI-DWI in breast cancer evaluated by two physicians (n = 63).

Observation item	MUSE-DWI			SS-EPI-DWI		
	ICC	*P* value	95%CI	ICC	*P* Value	95%CI
Image sharpness	0.857	< 0.01	(0.763–0.913)	0.818	< 0.01	(0.699–0.890)
Image artifact	0.856	< 0.01	(0.761–0.913)	0.852	< 0.01	(0.755–0.910)
Image distortion	0.709	< 0.01	(0.519–0.824)	0.883	< 0.01	(0.806–0.929)

Table 3
Comparison of subjective breast cancer scores between MUSE-DWI and SS-EPI-DWI (score, n = 63).

Image	image sharpness	image artifact	image distortion
Radiologist 1			
MUSE-DWI	4 (3,4)	3 (3,3)	3 (2,3)
SS-EPI-DWI	3 (3,4)	4 (3,4)	4 (3,4)
Z Value	−3.216	−4.709	−4.973
P Value	< 0.01	< 0.01	< 0.01
Radiologist 2			
MUSE-DWI	4 (3,4)	3 (3,4)	3 (2,4)
SS-EPI-DWI	3 (3,4)	4 (3,4)	4 (3,4)
Z Value	−4.310	−3.243	−3.978
P Value	< 0.01	< 0.01	< 0.01

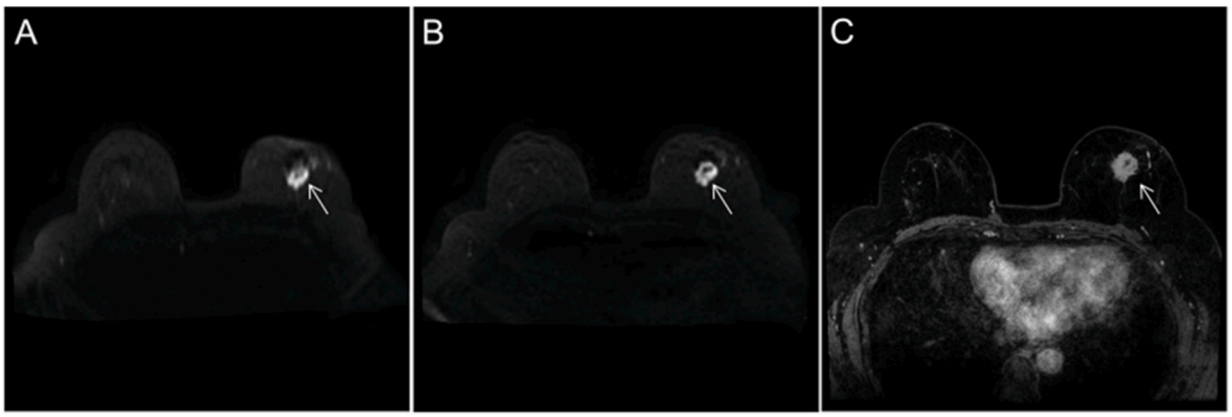

Fig. 3. A 56-year-old patient with grade NOS III invasive breast cancer. A. Breast axis SS-EPI-DWI. B. Axial MUSE-DWI C. Breast axial DCE-MRI. Compared with SS-EPI-DWI, MUSE-DWI can better display the lesions in the left breast mass, in which the central low-signal necrotic area can be clearly displayed, and the overall image quality is closer to that of DCE-MRI.

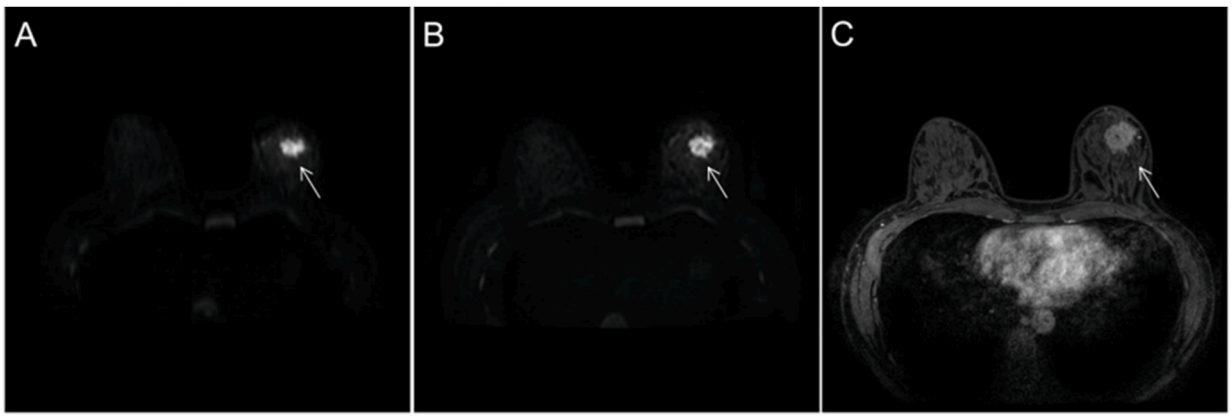

Fig. 4. A 36-year-old patient with grade NOS II invasive breast cancer. A. The axial SS-EPI-DWI of the breast is shown as B. Axial MUSE-DWI C. Breast axial DCE-MRI. In the left breast mass, MUSE-DWI can better display the lesion than SS-EPI-DWI, and the SS-EPI-DWI image distortion is more obvious when compared with DCE-MRI.

role in predicting the histological grade of invasive breast cancer [27]. In our study, the ADC values of grade III invasive breast cancer were lower than those of grades I and II, which aligns with the findings of Mori and others [28]. This observation may be due to the fact that higher-grade invasive breast cancers exhibit greater nuclear pleomorphism and higher mitotic counts, lack glandular and tubular structures, and have a denser internal arrangement. The ROC curve analysis further demonstrates that the ADC values derived from MUSE-DWI and single-shot DWI have AUC values of 0.849 and 0.801, respectively, in predicting the histological grade of invasive breast cancer. Although the predictive performance is not particularly striking, MUSE-DWI outperforms SS-EPI-DWI in terms of prediction accuracy. The integration of MUSE-DWI with multi-modal MRI or other techniques may further enhance the differentiation

Table 4
SNR comparison between MUSE-DWI and SS-EPI-DWI sequences.

Scan sequence	Mean	95 % CI	*T Test*	
			T Value	*P* value
MUSE-DWI	585.1 ± 224.9	(127.6,232.5)	6.869	*P* < 0.05
SS-EPR-DWI	405.0 ± 168.1			

Table 5
Comparison of ADC values between MUSE-DWI and SS-EPI-DWI sequences.

Scan sequence	Mean ($\times 10^{-6}$ mm^2/s)	95 % CI ($\times 10^{-6}$ mm^2/s)	*T Test*	
			T Value	*P* value
MUSE-DWI	0.82 ± 0.13	(-0.088 , -0.015)	−3.131	*P* < 0.05
SS-EPR-DWI	0.89 ± 0.15			

Table 6
Efficacy of MUSE-DWI and SS-EPI-DWI in predicting histological grading of invasive breast cancer.

Scan sequence	AUC	Sensitiv-ity (%)	Specific-ity (%)	maximum approxim-ate entry	index best bound	P Value
MUSE-DWI	0.849	74.6	89.5	0.64	0.89	< 0.05
SS-EPI-DWI	0.801	73.1	81.9	0.57	0.83	< 0.05

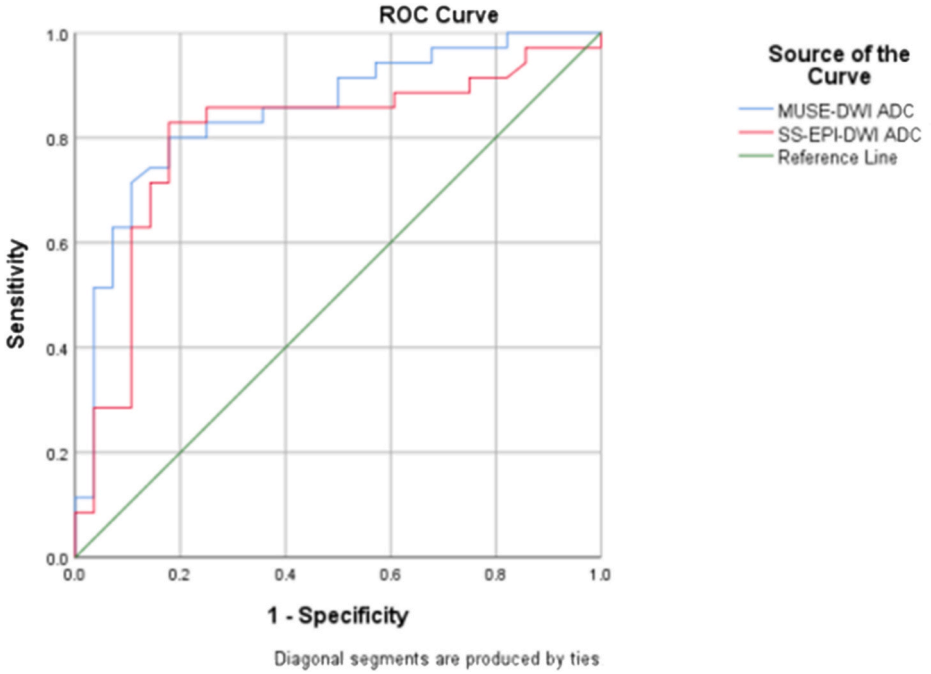

Fig. 5. ROC curve of MUSE-DWI ADC value and SS-EPI-DWI preoperative classification for predicting invasive breast cancer.

of histological grades in invasive breast cancer. Recurrence scores of grades I and II tumors are significantly lower than those of grade III [29,30]. Therefore, accurate preoperative prediction of the histological grade of invasive breast cancer is crucial for evaluating patient prognosis and recurrence. However, current histological grading relies on invasive biopsies, which are constrained in accuracy due to the complex heterogeneity of breast cancer [31].

There are several limitations in our study. Firstly, the small sample size may lead to potential bias.Secondly, our study focused solely on solid mass lesions, and future research should investigate the diagnostic value of MUSE-DWI in non-mass-like breast cancer. Additionally, the MUSE-DWI technique has limitations in terms of increased scan time with an increase in excitations. As such, the full potential of the MUSE-DWI sequence in the context of breast diseases remains to be explored and addressed in future studies. Future research should strive to further enhance the image quality of MUSE-DWI to achieve comparable results with contrast-enhanced

imaging, providing better visualization of breast cancer lesion contours without the necessity of contrast agents.

In conclusion, the results of our study demonstrate that high spatial resolution MUSE-DWI is feasible and can be seamlessly integrated into routine clinical breast MRI protocols. MUSE-DWI surpasses SS-EPI-DWI in terms of image quality and excels in predicting the histological grade of invasive breast cancer. Incorporating MUSE-DWI into clinical practice could transform breast cancer diagnosis, reducing the need for invasive biopsies, providing better visualization without contrast agents, and offering improved prognostic information.

Data availability

Data will be made available on request.

CRediT authorship contribution statement

Weicheng Wang: Writing – review & editing. **Bowen Dou:** Conceptualization. **Qi Wang:** Data curation. **Haogang Li:** Formal analysis. **Changshuai Li:** Project administration. **Wenjing Zhao:** Methodology. **Longjiang Fang:** Supervision. **Dmytro Pylypenko:** Writing – review & editing, Writing – original draft. **Yujing Chu:** Supervision, Resources, Project administration, Funding acquisition.

Declaration of competing interest

The authors declare that they have no known competing financial interests or personal relationships that could have appeared to influence the work reported in this paper.

References

[1] U. Veronesi, P. Boyle, A. Goldhirsch, R. Orecchia, G. Viale, Breast cancer, Lancet 365 (9472) (2005) 1727–1741.
[2] B. Weigelt, Reis-Filho JSHistological and molecular types of breast cancer: is there a unifying taxonomy? Nat. Rev. Clin. Oncol. 6 (12) (2009) 718–730.
[3] E.A. Rakha, M.E. El-Sayed, A.H. Lee, et al., Prognostic significance of Nottingham histologic grade in invasive breast carcinoma, J. Clin. Oncol. 26 (19) (2008) 3153–3158.
[4] H.J. Chon, W.J. Hyung, C. Kim, et al., Differential prognostic implications of gastric signet ring cell carcinoma: stage adjusted analysis from a single high-volume center in Asia, Ann. Surg. 265 (5) (2017) 946–953.
[5] L.W. Dalton, D.L. Page, W.D. Dupont, Histologic grading of breast carcinoma. A reproducibility study, Cancer 73 (11) (1994) 2765–2770.
[6] E.A. Rakha, M.E. El-Sayed, S. Menon, A.R. Green, A.H. Lee, I.O. Ellis, Histologic grading is an independent prognostic factor in invasive lobular carcinoma of the breast, Breast Cancer Res. Treat. 111 (1) (2008) 121–127.
[7] A.E. Giuliano, S.B. Edge, G.N. Hortobagyi, Eighth edition of the AJCC cancer staging manual: breast cancer, Ann. Surg Oncol. 25 (7) (2018) 1783–1785.
[8] R.M. Mann, N. Cho, L. Moy, Breast MRI: State of the Art, Radiology 292 (3) (2019) 520–536.
[9] T. Meng, N. He, H. He, et al., The diagnostic performance of quantitative mapping in breast cancer patients: a preliminary study using synthetic MRI, Cancer Imag. 20 (1) (2020) 88.
[10] B. Schmitt, S. Trattnig, H.P. Schlemmer, CEST-imaging: a new contrast in MR-mammography by means of chemical exchange saturation transfer, Eur. J. Radiol. 81 (Suppl 1) (2012) S144–S146.
[11] S.C. Partridge, N. Nissan, H. Rahbar, A.E. Kitsch, E.E. Sigmund, Diffusion-weighted breast MRI: clinical applications and emerging techniques, J. Magn. Reson. Imag. 45 (2) (2017) 337–355.
[12] M. Iima, M. Honda, E.E. Sigmund, A. Ohno Kishimoto, Togashi K. Kataoka, Diffusion MRI of the breast: current status and future directions, J. Magn. Reson. Imag. 52 (1) (2020) 70–90.
[13] C. Spick, H. Bickel, K. Pinker, et al., Diffusion-weighted MRI of breast lesions: a prospective clinical investigation of the quantitative imaging biomarker characteristics of reproducibility, repeatability, and diagnostic accuracy, NMR Biomed. 29 (10) (2016) 1445–1453.
[14] D.J. Wisner, N. Rogers, V.S. Deshpande, et al., High-resolution diffusion-weighted imaging for the separation of benign from malignant BI-RADS 4/5 lesions found on breast MRI at 3T, J. Magn. Reson. Imag. 40 (3) (2014) 674–681.
[15] G.C. Baxter, A.J. Patterson, R. Woitek, I. Allajbeu, M.J. Graves, F. Gilbert, Improving the image quality of DWI in breast cancer: comparison of multi-shot DWI using multiplexed sensitivity encoding to conventional single-shot echo-planar imaging DWI, Br. J. Radiol. 94 (1119) (2021) 20200427.
[16] J. Li, Y.C. Bai, L.H. Wu, et al., Synthetic relaxometry combined with MUSE DWI and 3D-pCASL improves detection of hippocampal sclerosis, Eur. J. Radiol. 157 (2022) 110571.
[17] T. Ota, T. Tsuboyama, H. Onishi, et al., Diagnostic accuracy of MRI for evaluating myometrial invasion in endometrial cancer: a comparison of MUSE-DWI, rFOV-DWI, and DCE-MRI published online ahead of print, 2023 Apr 29, Radiol. Med. (2023), https://doi.org/10.1007/s11547-023-01635-4.
[18] H.C. Chang, G. Chen, H.W. Chung, et al., Multi-shot diffusion-weighted MRI with multiplexed sensitivity encoding (MUSE) in the assessment of active inflammation in Crohn's disease, J. Magn. Reson. Imag. 55 (1) (2022) 126–137.
[19] O. Dietrich, J.G. Raya, S.B. Reeder, M.F. Reiser, S.O. Schoenberg, Measurement of signal-to-noise ratios in MR images: influence of multichannel coils, parallel imaging, and reconstruction filters, J. Magn. Reson. Imag. 26 (2007) 375–385.
[20] G.E. Park, S.H. Kim, E.J. Kim, B.J. Kang, M.S. Park, Histogram analysis of volume-based apparent diffusion coefficient in breast cancer, Acta Radiol. 58 (11) (2017) 1294–1302.
[21] H. Takahashi, M. Oshi, M. Asaoka, L. Yan, I. Endo, K. Takabe, Molecular biological Features of Nottingham histological grade 3 breast cancers, Ann. Surg Oncol. 27 (11) (2020) 4475–4485.
[22] D.V. Cicchetti, Guidelines,Criteria,and rules of thumb for evaluating normed and standardized assessment instruments in psychology, [J].Psychological Assessment 6 (4) (1994).
[23] I. Daimiel Naranjo, R. Lo Gullo, E.A. Morris, et al., High-spatial-resolution multishot multiplexed sensitivity-encoding diffusion-weighted imaging for improved quality of breast images and differentiation of breast lesions: a feasibility study, Radiol Imaging Cancer 2 (3) (2020) e190076.
[24] Y. Hu, D.M. Ikeda, S.M. Pittman, et al., Multishot diffusion-weighted MRI of the breast with multiplexed sensitivity encoding (MUSE) and shot locally low-rank (Shot-LLR) reconstructions, J. Magn. Reson. Imag. 53 (3) (2021) 807–817.
[25] H.C. Chang, P. Gaur, Y.H. Chou, M.L. Chu, N.K. Chen, Interleaved EPI based fMRI improved by multiplexed sensitivity encoding (MUSE) and simultaneous multi-band imaging, PLoS One 9 (12) (2014) e116378.
[26] R. Bammer, S.L. Keeling, M. Augustin, et al., Improved diffusion-weighted single-shot echo-planar imaging (EPI) in stroke using sensitivity encoding (SENSE), Magn. Reson. Med. 46 (3) (2001) 548–554.

[27] A. Surov, D.T. Ginat, T. Lim, et al., Histogram analysis parameters apparent diffusion coefficient for distinguishing high and low-grade meningiomas: a multicenter study, Transl Oncol 11 (5) (2018) 1074–1079.
[28] N. Mori, C. Inoue, H. Tamura, et al., Apparent diffusion coefficient and intravoxel incoherent motion-diffusion kurtosis model parameters in invasive breast cancer: correlation with the histological parameters of whole-slide imaging, Magn. Reson. Imaging 90 (2022) 53–60, https://doi.org/10.1016/j.mri.2022.04.003.
[29] Z. Ping, Y. Xia, T. Shen, et al., A microscopic landscape of the invasive breast cancer genome, Sci. Rep. 6 (2016) 27545. Published 2016 Jun 10.
[30] M. Gerlinger, A.J. Rowan, S. Horswell, et al., Intratumor heterogeneity and branched evolution revealed by multiregion sequencing published correction appears in N Engl J Med. 2012 Sep 6;367(10):976], N. Engl. J. Med. 366 (10) (2012) 883–892.
[31] N.K. Chen, A. Guidon, H.C. Chang, A.W. Song, A robust multi-shot scan strategy for high-resolution diffusion weighted MRI enabled by multiplexed sensitivity-encoding (MUSE), Neuroimage 72 (2013) 41–47.